Formation of New Glucomannan−Chitosan Nanoparticles and Study of Their Ability To Associate and Deliver Proteins

María Alonso-Sande,[†] Margarita Cuña,[†] Carmen Remuñán-López,[†] Desirée Teijeiro-Osorio,[†] José L. Alonso-Lebrero,[‡] and María J. Alonso*,[†]

Department of Pharmaceutical Technology, Faculty of Pharmacy, University of Santiago de Compostela, Spain, and R&D Department, Industrial Farmacéutica Cantabria SA, Spain

Received January 30, 2006; Revised Manuscript Received April 10, 2006

ABSTRACT: The purpose of this work was to investigate the factors involved in the formation of a new type of nanoparticle made of hydrophilic polysaccharides, chitosan (CS), and glucomannan (GM) and to study their potential for the association and delivery of proteins. Two different types of glucomannan were used (non-phosphorylated Konjac GM (KGM) and phosphorylated GM), and two different approaches were adopted for the preparation of the nanoparticles. These procedures involved the interaction of CS and GM in the presence or absence of sodium tripolyphosphate, which acted as an ionic cross-linking agent for CS. Using both approaches, it was possible to obtain nanoparticles with a size in the range from 200 to 700 nm and a variable zeta potential (from −2 to +39 mV), depending on the formulation conditions. Despite the mild forces involved in their formation, by adjusting the process variables, it was also possible to obtain nanoparticles that remain stable upon dilution with phosphate buffer saline. The nanoparticles exhibited a great capacity for the association of the model peptide insulin and the immunomodulatory protein P1, reaching association efficiency values as high as 89%. Moreover, the release of the peptide/protein could be modulated by varying the composition of the system. Consequently, the results presented here suggest that chitosan−glucomannan nanoparticles are promising carriers for the oral administration of peptides and proteins.

1. Introduction

A major recent challenge confronted in pharmaceutical sciences has been the development of effective delivery systems especially adapted for transmucosal administration of peptides and proteins.[1] Indeed, the efficacy of these active macromolecules is strongly hampered not only by their chemical and physical instability but also by the high metabolic activity and the limited permeability of the mucosal barriers.[2] As a consequence, the future of these molecules as therapeutic agents clearly depends on the design of appropriate vehicles for their delivery to the body. Several strategies have been explored so far to overcome these limitations, among which the design of biodegradable poly(lactic acid−glycolic acid) PLGA nanoparticles has attracted considerable interest.[3] However, an inconvenience of these particles is that their preparation requires the use of aggressive conditions (organic solvents, sonication, etc.) that compromise the stability of the encapsulated molecules. In addition, the degradation of these particles occurs over long periods of time, a situation that contributes to the degradation of the encapsulated protein.

An interesting alternative to hydrophobic nanoparticles is that made of hydrophilic polymers such as the polysaccharide CS. CS has a well-documented biocompatibility and low toxicity;[4,5] it adheres to the mucosal surfaces[6] and has the capacity of promoting the permeation of macromolecules through well-organized epithelia (nasal, intestinal, ocular, buccal).[7−10] The potential of CS for this specific application has been further reenforced by its demonstrated ability to form colloidal particles which entrap macromolecules through a number of mechanisms, including ionic cross-linking, desolvation, or ionic complexation.[11] In this respect, we have recently reported the preparation of CS nanoparticles via a mild ionotropic gelation procedure with the counterion sodium tripolyphosphate (TPP).[12,13] These nanoparticles have shown a high capacity for the association of macromolecules such as insulin, BSA, tetanus toxoid, and diphtheria toxoids. Moreover, in vivo experiments have evidenced their potential as nasal carriers for peptides and antigens.[8,14]

Based on this previous information, the aim of this paper was to develop a new nanoparticulate system, made of CS and GM, exhibiting adequate properties for the oral administration of peptides and proteins. The polysaccharide GM—either in a noncharged form (KGM) or negatively charged form (phosphorylated GM)—was chosen as a second ingredient for the nanoparticles formation because of its ability to interact with CS. Moreover, an interesting characteristic of GM relies on its ability to interact favorably with some biological surfaces which are particularly rich in mannose receptors, such as the M-cells overlying the Peyer's patches[15] and macrophages.[16] In addition, it has been reported that the addition of GM to CS gels may help in enhancing the stability of the resulting systems in the gastrointestinal fluids.[17,18] Therefore, based on this previous information, our hypothesis was that the nanoparticles made of CS and GM would be adequate vehicles for the delivery of peptides/proteins across the intestinal epithelium and, in particular, through the M-cells overlying Peyer's patches.

In light of these considerations, we first aimed at finding the adequate conditions for the formation of the particles and, second, we investigated their potential for the association and release of proteins. For this latter purpose, we chose insulin and an immunomodulatory protein (P1). P1 is a mixture of polypeptides which have shown the ability to up-regulate natural and specific cell-mediated immune mechanism, thus having application in therapeutic treatment of intra- and extracellular infections and as vaccination adjuvant.[19]

[†] University of Santiago de Compostela.
[‡] Industrial Farmacéutica Cantabria SA.
* To whom correspondence should be addressed: Ph 00 34 981 563100-14885; Fax 00 34 981 547148; e-mail ffmjalon@usc.es.

10.1021/ma060230j CCC: $33.50
Published on Web 05/17/2006

2. Materials and Methods

2.1. Materials. Chitosan (CS) in the form of hydrochloride salt [Protasan Cl 110; supplier's specifications: intrinsic viscosity at 25 °C = 10 mPa, M_w = 110 kDa, deacetylation degree = 87%] was provided by Pronova Biopolymer (Norway). Konjac glucomannan (KGM) [RX-L; supplier's specifications: intrinsic viscosity at 25 °C = 15000 ± 5000 mPa] was purchased by Shimizu Chemical Co. (Japan). Phosphorylated GM [supplier's specifications: mannose = 84%, glucose and phosphate groups = 7 ± 3%, M_w = 150 kDa] and P1 [immunomodulatory mixture of proteins; supplier's specifications: M_w = 8−12 kDa, isoelectric point (IP) = 3−9] were kindly supplied by Industrial Farmacéutica Cantabria (Madrid, Spain). Bovine insulin [supplier's specifications: M_w = 5.8 kDa, IP = 5.3], pentasodium tripolyphosphate (TPP), and glycerol were purchased from Sigma Chemical Co. (Spain). Ultrapure water [Milli-Q Plus, Millipore Ibérica, Spain] was used throughout. All other reagents were analytical grade.

2.2. Preparation of Polymer Solutions. CS solutions (2 or 3 mg/mL) were prepared by dissolving the polymer in either purified water or acetic acid 1% (v/v) for 2 h under magnetic stirring. The pH of the CS solutions was adjusted to 4.8 by adding NaOH (10 M). Phosphorylated GM was dissolved in pure water at the concentration of 23 mg/mL, obtaining a final pH of 7.1. Non-phosphorylated KGM was first dispersed in water; then, the suspension was centrifuged, and the supernatant was freeze-dried and dissolved at 1 mg/mL in 10 mM Na_2HPO_4 (pH: 8.26) to obtain a clear solution (viscosity of 1% (w/v) solution in water at 25 °C = 1291 ± 36 mPa·s; experimentally determined with a Oswald's viscosimeter). Finally, TPP was directly dissolved in pure water at the concentrations of 0.84 or 3.3 mg/mL, depending on the formulation.

2.3. Preparation of Nanoparticles. We adopted two different approaches for the preparation of the nanoparticles. First, we prepared nanoparticles made of solely CS and GM (CS-KGM and CS-phosphorylated GM nanoparticles) upon mixing the aqueous solutions of both polymers. In a second approach, we prepared CS/TPP-GM nanoparticles by a previously described ionotropic gelation method within CS and TPP,[12] which here was modified to incorporate either KGM or phosphorylated GM into the nanoparticles structure.

Preparation of CS−GM Nanoparticles. CS−phosphorylated GM nanoparticles of 6/4.6 and 6/13.8 theoretical CS/phosphorylated GM ratios were formed spontaneously upon the incorporation of prefixed volumes (0.2 and 0.6 mL) of the phosphorylated GM solution (23 mg/mL in pure water, pH 7.1) onto 3 mL of the CS solution (2 mg/mL in pure water, pH 4.7) under magnetic stirring at room temperature. As indicated above, CS was directly dissolved in pure water or in acetic acid solution 1% (v/v) followed by raising the pH up to 4.8 by adding NaOH 10 M. On the other hand, CS−KGM nanoparticles of 6/4.6, 6/6, 6/12, 6/13.8, 6/18, and 6/24 theoretical CS/KGM ratios were obtained upon the addition of 1.15 and 6 mL of the KGM (non-phosphorylated) solution to 0.5 mL of the CS solution (3 mg/mL, in pure water, pH 4.75). Thereafter, the nanoparticles were purified by centrifugation (10000*g*, 40 min, 4 °C; Beckman Avanti 30, Beckman) using a bed made of 20 μL of glycerol. The supernatants were discarded, and the nanoparticles reconstituted in 100−200 μL of pure water.

Preparation of CS/TPP-GM Nanoparticles. Nanoparticles of a 6/1 theoretical CS/TPP ratio were formed spontaneously upon the incorporation of 1.2 mL of TPP solution (0.84 mg/mL) into 3 mL of a CS aqueous solution (2 mg/mL) under mild magnetic stirring, at room temperature. These nanoparticles were used as control.

For the preparation of CS/TPP−phosphorylated GM and CS/TPP−KGM, the polymer solutions were prepared as indicated before. CS/TPP−phosphorylated GM nanoparticles of 6/1/2.3 and 6/1/4.6 theoretical CS/TPP/phosphorylated GM ratios were obtained by incorporating 100 and 200 μL of a phosphorylated GM aqueous solution (23 mg/mL) to 1.2 mL of the TPP (0.84 mg/mL) aqueous phase before the nanoparticles formation. CS/TPP-KGM nanoparticles of 6/1/1.2, 6/1/1.8, 6/1/2.3, 6/1/3, and 6/1/4.6 theoretical CS/TPP/KGM ratios were formed upon the addition of a mixture of KGM and TPP (KGM = 1 mg/mL, 1.2−4.6 mL; TPP = 3.3. mg/mL, 0.3 mL) into 3 mL of CS solution (2 mg/mL) under magnetic stirring at room temperature. Thereafter, the nanoparticles were purified as described before.

2.4. Association of Insulin and P1 Protein to the Nanoparticles. Insulin was dissolved at a concentration of 5 mg/mL in NaOH 0.01 M (pH 11), and P1 protein was dissolved at 7.7 mg/mL in 10 mM phosphate buffer (pH 6.6). Then the insulin and P1 protein solutions (0.6 and 0.3 mL, respectively) were added to the TPP and/or GM solutions for the CS/TPP−GM and CS−GM formulations, respectively. Protein theoretical loadings were calculated to obtain CS/insulin and CS/P1 protein ratios of 2/1−2.4/1 and 1.6/1−2.2/1, respectively, which correspond to theoretical loadings of 20−22% (w/w) for insulin and 16−21% (w/w) for protein P1. The nanoparticles containing insulin and P1 protein were prepared according to the procedures indicated before.

2.5. Determination of Process Yield. For the calculation of the nanoparticles production yields, the nanoparticles suspension were centrifuged (10000*g*, 4 °C, 40 min), and the supernatant was discarded. The tubes containing the sediments were freeze-dried for 24 h, and the difference of the theoretical solids weights and the actual freeze-dried nanoparticles weights were obtained (n = 3). The yield of the process was calculated as follows:

$$\text{process yield (\%)} = \frac{\text{nanoparticles weight}}{\text{total solids (CS + TTP + GM) weight}} \times 100$$

2.6. Characterization of Nanoparticles. The morphological examination of the nanoparticles was performed by transmission electron microscopy (TEM) (CM12 Philips, Eindhoven, The Netherlands). The samples were stained with 2% w/v phosphotungstic acid for 10 s, immobilized on copper grids with Formvard, and dried overnight for viewing by TEM.

The measurements of size and zeta potential of the nanoparticles were performed by photon correlation spectroscopy and laser Doppler anemometry, respectively, with a Zetasizer 3000HS (Malvern Instruments, Malvern, UK). For the determination of the zeta potential, samples were diluted in 1 mM KCl and measured in automatic mode (placed in the electrophoretic cell where a potential of ±150 mV was established). The zeta potential values were calculated from the mean electrophoretic mobility values using the Smoluchowski's equation. For size analysis, samples were diluted in water and measured for a minimum of 18 s. Raw data were subsequently correlated to mean hydrodynamic size by cumulative analysis ($n \geq 6$).

2.7. Evaluation of Nanoparticles Stability. The stability of the nanoparticles was investigated in phosphate buffer saline (PBS) pH 7.4 at room temperature. Aliquots of fresh suspensions of nanoparticles were diluted with PBS, reaching a concentration 1 mg/mL, and the evolution of size was assessed using photon correlation spectroscopy (Zetasizer 3000HS, Malvern Instruments, UK) for 2 h at room temperature (n = 4).

2.8. Determination of Protein Loading Capacity of Nanoparticles. The quantity of insulin and P1 protein entrapped in the nanoparticles was calculated by the difference between the total protein incorporated in the nanoparticles formation medium and the quantity of nonentrapped protein remaining in the aqueous suspending medium. Association efficiencies of the nanoparticles were determined upon their separation from aqueous suspension medium by centrifugation (10000*g*, 4 °C, 40 min). Insulin and P1 protein were analyzed in the supernatant by Micro BCA protein assay at 562 nm (Pierce, Rockford, IL). Calibration curves were made with corresponding solutions of blank nanoparticles (n = 4).

The protein association efficiency and protein loading capacity of the nanoparticles were calculated as follows:

$$\text{association efficiency (\%)} = \frac{\text{total protein (mg)} - \text{free protein (mg)}}{\text{total protein (mg)}} \times 100$$

$$\text{loading capacity (\%)} = \frac{\text{total protein (mg)} - \text{free protein (mg)}}{\text{nanoparticles weight}} \times 100$$

2.9. In Vitro Release Studies. The releases of insulin and P1 protein from the nanoparticles were determined by incubating the nanoparticles in 1.5 and 1 mL (1−0.5 mg of nanoparticles), respectively, of pH 7.4 phosphate buffer (PBS) at 37 °C (P-Selecta, Hotcold-M, Spain) under mild horizontal agitation (Promax 1020, Heidolph, Germany). At appropriate time intervals, the individual samples were filtered and supernatants isolated, and released protein was evaluated by the Micro BCA protein assay (Pierce, Rockford, IL). A calibration curve was made at each time interval using nonloaded nanoparticles ($n = 4$).

3. Results and Discussion

3.1. Formation and Characterization of Nanoparticles. In this work, we report the preparation and characterization of new nanoparticulate systems consisting of two polysaccharides, CS and GM (Figure 1), which were obtained under exceptionally mild conditions. As stated in the Introduction, we have previously reported the development of CS nanoparticles based on the ionic cross-linking of CS with a counterion such as TPP.[12] The intra- and intermolecular linkages created between the negative groups of TPP and the positively charged amino groups of CS were responsible for the success of the process. These nanoparticles have shown a potential for nasal administration of proteins.[8,14] In the present work, the introduction of GM as a second ingredient in the nanoparticulate formulation was expected to open new possibilities for their interaction with biological surfaces.[15] With this idea in mind, we have developed a number of approaches for the preparation of nanoparticles containing CS and GM, based on mixing aqueous phases at room temperature. These approaches involve (i) mixing an aqueous phase containing CS with an aqueous phase that contains the cross-linking agent TPP (formation of CS/TPP nanoparticles) followed by their coating with GM or alternatively (ii) mixing an aqueous phase containing CS with an aqueous phase that contains GM with or without the cross-linking agent TPP. In a previous article we reported the results corresponding to the first approach and the efficient association of proteins to the nanoparticles.[20] In this work, we present the results corresponding to the second alternative. The GM used to form the nanoparticles was either KGM, obtained from *Amorphophallus konjac*, or phosphorylated GM, isolated from the cell wall of *Candida utilli*s. As previously reported, both polysaccharides, CS and GM, were expected to interact through intermolecular hydrogen bonds in addition to the electrostatic interactions.[17,18] However, the phosphate groups (negatively charged) of phosphorylated GM were expected to facilitate the ionic interaction of this GM with the positively charged CS molecules. The differences in the chemical structure of both types of GM are shown in Figure 1.

CS−GM Nanoparticles. To begin, we conducted a study in order to identify the adequate processing conditions for the formation of nanoparticles made of solely CS and GM (phosphorylated or not). Taking into account the negative charge of the phosphorylated GM, it was expected that, under the appropriate conditions, it could electrostatically interact with CS, leading to the formation of CS-phosphorylated GM nanoparticles. In fact, nanoparticles with 6/4.6 and 6/13.8 theoretical CS/phosphorylated GM ratios were obtained upon mixing a CS solution (in water or acetic acid), with an aqueous solution of phosphorylated GM. The physicochemical properties of fresh CS−phosphorylated GM nanoparticles are shown in Table 1. Higher process yields were obtained for the nanoparticles

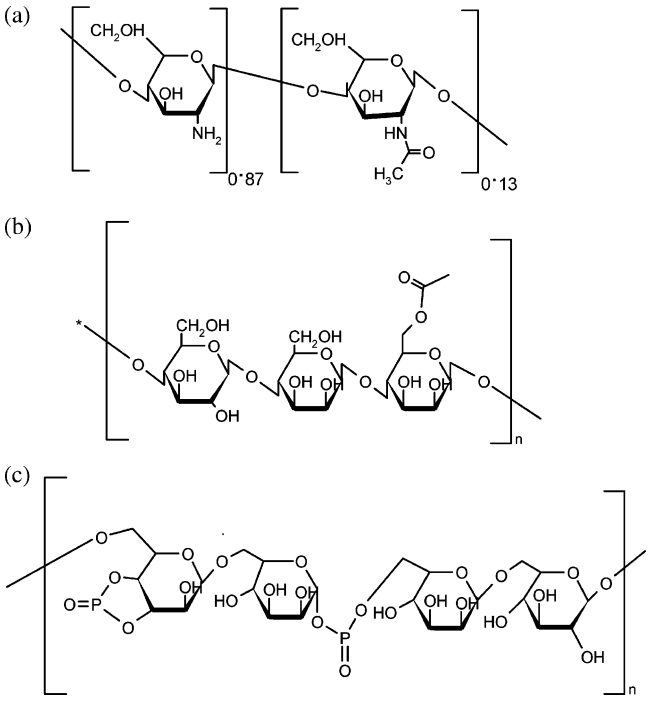

Figure 1. Chemical structure of (a) CS, (b) KGM, and (c) phosphorylated GM polymers.

Table 1. Physicochemical Properties of CS−Phosphorylated GM Nanoparticles Prepared with Different CS/Phosphorylated GM Theoretical Ratios (Mean ± SD, $n = 6$)

CS/phosphorylated GM (w/w)	process yield (%)	size (nm)	ζ potential (mV)
6/4.6[a]	22 ± 5	252 ± 15	+31.25 ± 1.0
6/13.8[a]	20 ± 3	183 ± 02	+30.5 ± 0.2
6/4.6[b]	45 ± 3	300 ± 12	+33.6 ± 1.0
6/13.8[b]	54 ± 3	185 ± 04	+33.2 ± 0.8

[a] CS was dissolved in pure water (final pH: 4.8). [b] CS was dissolved in acetic acid and neutralized up to pH 4.8 by adding NaOH (10 M) prior to mixing with phosphorylated GM.

prepared using CS solutions in acetic acid as compared to those obtained with CS solutions in water. This could be related to the higher ionic strength created by the presence of sodium acetate (the CS acetic acid solution was neutralized with NaOH). Several authors have described the effect of ionic strength on the conformation of the CS chains, which is related with the variation of the electrostatic charges along the polymer chains.[21,22] Furthermore, the ionic strength has a significant effect on the intrinsic viscosity (particularly at low salt levels), increasing polymer chain flexibility,[23] which could improve the interaction between both polymers (CS and phosphorylated GM). On the other hand, the results of the process yield shown in Table 1 indicate that an increase in the amount of phosphorylated GM led to the formation of a greater number of particles. This effect, only apparent for the formulations prepared in the presence of sodium acetate, could be attributed to the nanoparticles formation mechanism. As indicated above, the ionic strength may improve hydrophobic polymer−polymer interaction and, hence, increase the incorporation of GM into the nanoparticles.

The results in Table 1 also indicate that the nanoparticles have a size ranging from approximately 180 to 310 nm, depending on polymer composition (CS/phosphorylated GM ratio): an increase in the content of phosphorylated GM led to a smaller size. This size reduction could be explained by the compaction of the nanoparticles structure following the CS−anionic GM interaction. Decreasing the amount of phosphory-

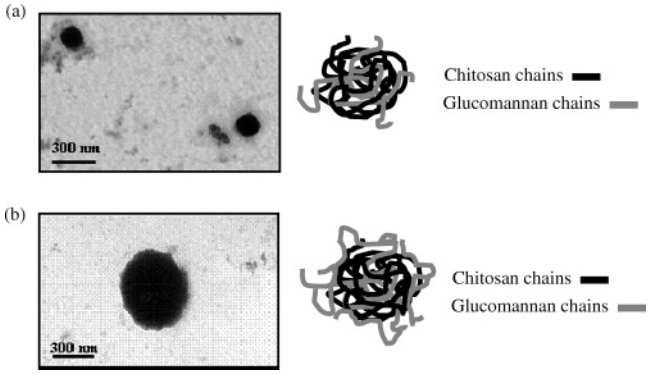

Figure 2. TEM microphotographs and expected structure of CS/GM nanoparticles made with different compositions. Nanoparticles polymer composition: (a) CS/phosphorylated GM(6/4.6) (× 75K); (b) CS/KGM (6/6) (× 60K).

Table 2. Physicochemical Properties of CS−KGM Nanoparticles Prepared with Different CS/KGM Theoretical Ratios (Mean ± SD, $n = 12$)

CS[a]/KGM (w/w)	process yield (%)	size (nm)	ζ potential (mV)
6/6	45 ± 2	745 ± 36	−0.8 ± 0.4
6/12	44 ± 4	611 ± 19	−0.4 ± 0.4
6/13.8	40 ± 2	588 ± 20	−1.65 ± 1.1
6/18	36 ± 2	493 ± 03	−2.2 ± 0.1
6/24	28 ± 4	488 ± 20	−2.1 ± 0.2

[a] CS was dissolved in water.

lated GM implies a reduction in the number of anions that are available to neutralize the amino groups of CS and, hence, to condense the polymer into tight particles.[24] Interestingly, despite the effect of the GM content on the size of the particles, the positive values of zeta potential (above +30 mV) were not substantially affected by the CS/phosphorylated GM ratio. This could be explained by the important positive charge density of CS as compared to that of phosphorylated GM. In fact, while around 87% of amino groups are expected to be positively charged in each CS molecule, only 7% of the OH groups of the phosphorylated GM were phosphorylated. This conclusion agrees with that reported by Du et al.,[25] who found that the superficial charge of CS/carboxymethyl GM nanoparticles were not influenced by the GM content. Illustrations of the expected and obtained structure for CS−phosphorylated GM nanoparticles by TEM are presented in Figure 2a.

In the first step of this work we assumed that the presence of the phosphate group in the phosphorylated GM would be critical in the formation of the nanoparticles; however, as illustrated in Figure 2b, CS−GM nanoparticles could also be obtained upon mixing of CS and KGM (non-phosphorylated) solutions in adequate conditions. More specifically, nanoparticles could be obtained with CS/KGM theoretical ratios from 6/6 to 6/24. In this case, the mechanism of nanoparticles formation is probably due to the already mentioned intermolecular hydrogen bonds within the hydroxyl groups of KGM and the free amino groups of CS.[17] As shown in Table 2, the highest process yields were obtained for the nanoparticles from 6/6 to 6/13.8 theoretical CS/KGMratios. A further increase in the amount of KGM and, hence, in theoretical total solids content led to a decrease in the process yield. This could be attributed to the fact that there is an excess of KGM, which cannot be integrated into the nanoparticle structure.

As noted for CS-phosphorylated GM nanoparticles, the increase of the KGM content led to the condensation of the nanostructure and hence to the reduction of the particle size. However, the size of CS−KGM nanoparticles (470−800 nm)

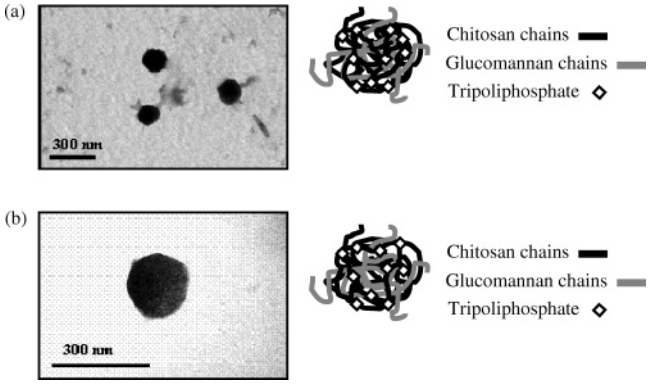

Figure 3. TEM microphotographs and expected structure of CS/TPP/GM nanoparticles made with different compositions. Nanoparticles polymer composition: (a) CS/TPP/phosphorylated GM (6/1/4.6) (× 75K); (b) CS/TPP/KGM (6/1/1.8) (× 260K).

was larger than that of the particles containing phosphorylated GM (Table 1). This result could be related to the different interaction forces between the two interacting species (CS and KGM), leading to a lower degree of compaction of the resulting nanostructure. This interpretation is in agreement with that given by Xu et al.[26] for the larger size of CS/TPP/PEG nanoparticles as compared to CS/TPP−sodium alginate nanoparticles. They attributed these differences to the weaker interaction between CS and PEG in comparison with the interaction of CS with sodium alginate. Nevertheless, although a different interaction could be expected for phosphorylated and non-phosphorylated KGM with CS, we cannot discard the potential influence of the GM molecular weight, which was much smaller for phosphorylated GM than for the non-phosphorylated KGM. In fact, it has been widely reported that the particle size of colloids, made by complexation of two polysaccharides, is highly influenced by the molecular weight of the initial components.[12,24,27]

With regard to the results of the surface charge, in contrast with those obtained for CS−phosphorylated GM nanoparticles (Table 1), the zeta potential values of the CS−KGM nanoparticles were neutral irrespective of the CS/KGM ratio. The neutral charge of the particles can only be explained by a shield effect of the KGM molecules (without charge) surrounding the positively charged CS molecules (see illustration in Figure 2b). This specific organization may be related to the formation process of the nanoparticles. In fact, we observed that whereas CS−phosphorylated GM nanoparticles formed spontaneously, CS−KGM nanoparticles need more time for their formation (15 min). This kinetics of particle formation and the structural organization of the two polysaccharides could be related not only to the different charge of both varieties of GM but also to their molecular weight. Furthermore, similar structures were described by Schatz et al.[27] for the formation of CS complexes with high molecular weight dextran sulfate. In actuality, they reported the formation of particles consisting in a hydrophobic core, made of CS and dextran sulfate, and a large hydrophilic shell of uncomplexed dextran sulfate segments.

CS/TPP−GM Nanoparticles. A substantial difference of these particles as compared to those described above is the incorporation of an ionic cross-linking agent, TPP, for CS. The TEM photographs of the CS/TPP−phosphorylated GM and CS/TPP−KGM nanoparticles are shown in parts a and b of Figure 3, and their physicochemical properties are depicted in Tables 3 and 4, respectively. The results in Table 3 show that the incorporation of phosphorylated GM into the nanoparticles did not cause a significant modification in the particle size or in process yield. These results could be explained because the

Table 3. Physicochemical Properties of CS/TPP−Phosphorylated GM Nanoparticles Prepared with Different CS/TPP/Phosphorylated GM Theoretical Ratios (Mean ± SD, $n = 6$)

CS[a]/TPP/phosphorylated GM (w/w/w)	process yield (%)	size (nm)	ζ potential (mV)
6/1/0[b]	35 ± 4	297 ± 25	+38.9 ± 0.3
6/1/2.3	31 ± 8	250 ± 24	+32.2 ± 2.0
6/1/4.6	39 ± 7	302 ± 26	+15.2 ± 1.7

[a] CS was dissolved in water. [b] Control (CS/TPP nanoparticles, without GM).

Table 4. Physicochemical Properties of CS/TPP−KGM Nanoparticles Prepared with Different CS/TPP/KGM Ratios (Mean ± SD, $n = 6$)

CS[a]/TPP/KGM (w/w/w)	process yield (%)	size (nm)	ζ potential (mV)
6/1/1.2	24 ± 2	318 ± 5	+31.4 ± 0.4
6/1/1.8	21 ± 8	304 ± 9	+29.6 ± 0.6
6/1/2.3	24 ± 4	303 ± 8	+25.3 ± 2.4
6/1/3	49 ± 8	465 ± 11	+14.1 ± 1.2

[a] CS was dissolved in water.

low amount of phosphorylated GM incorporated into the nanoparticle. In contrast, phosphorylated GM content strongly affected the zeta potential, which went from +38.9 to +15.2 mV. This surface charge reduction, which was not seen in the particles without TPP (Table 1), could be due to the different mechanism of particles formation. In this case, TPP is involved in the particle formation by ionic cross-linking; consequently, phosphorylated GM molecules may be consumed not only in particle formation but also in the neutralization of the free positive amino groups remaining in the CS/TPP nanoparticles (see illustration in Figure 3a).

From the comparison of the results in Tables 1 and 3, we can conclude that similar sizes were obtained for CS/TPP−phosphorylated GM and CS−phosphorylated GM nanoparticles with the same 6/4.6 CS/phosphorylated GM theoretical ratio. In contrast, the presence of TPP caused an increase of the yield (22 ± 5% vs 39 ± 7%), which could be explained by the presence of both types of counterion, TPP and phosphorylated GM, involved in the formation of more particles.

CS/TPP−KGM nanoparticles were obtained with several amounts of non-phosphorylated KGM. The physicochemical characteristics of the formulations are depicted in Table 4. For low KGM contents (CS/TPP/KGM: 6/1/1.2, 6/1/1.8, and 6/1/2.3), the sizes were around 300 nm; however, a significant increase in size was observed for a CS/TPP/KGM theoretical ratio of 6/1/3. Moreover, when the amount of KGM increases up to above the ratio of 6/1/4.6, large microparticles, other than nanoparticles, were formed (data not shown). This increase in the size, originated by the addition of important amounts of KGM, could be related to the entrapment of a greater amount of KGM within the particles gelled by the action of TPP. This explanation agrees with the more important process yield and the significant reduction of the surface change as the KGM content increased.[13] An illustration of the obtained structure by TEM is provided in Figure 3b. From the comparison of the results summarized in Tables 2 and 4 (corresponding to nanoparticles obtained with non-phosphorylated KGM, in the absence or presence of TPP, respectively), it can be concluded that the presence of TPP contributes to the formation of more compacted systems, of reduced particle size. This could be attributed to the different mechanism involved in the nanoparticle formation. In fact, the presence of TPP might lead to a more organized structure in which TPP reacts with CS, and KGM is incorporated into the network (Figure 3b). Furthermore,

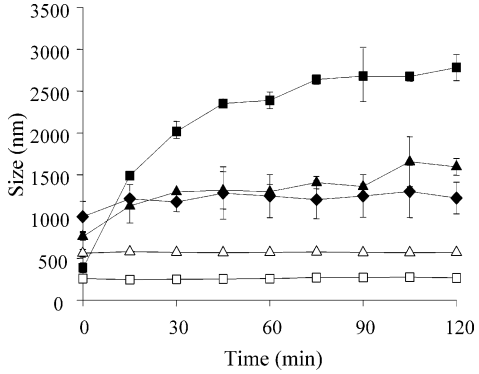

Figure 4. Evolution of the nanoparticles size following their incubation in PBS pH 7.4 up to 2 h at room temperature (mean ± SD, $n = 4$). Nanoparticles polymer composition: (▲) CS/phosphorylated GM (6/4.6); (◆) CS/phosphorylated GM (6/13.8); (■) CS/TPP/phosphorylated GM (6/1/4.6); (△) CS/KGM (6/6); (□) CS/TPP/KGM (6/1/1.8).

this organization of the polymers in the presence of TPP could also explain the positive charge of CS/TPP−KGM nanoparticles compared to CS−KGM ones (Table 2). Finally, the differences on the process yield obtained for both types of nanoparticles (CS/TPP−KGM and CS−KGM nanoparticles) could be related with the higher KGM content in CS−KGM formulations.

3.2. Stability Study of the Nanoparticles. An important goal when designing colloidal drug carriers, especially those prepared by mild ionic cross-linking processes, is to achieve an acceptable stability in high ionic strength media, similar to those present in the organism. In this regard, several authors have described that the combination of different polysaccharides, such as CS, GM, or alginate, could help to maintain the integrity of the resulting systems.[18,28,29] In the present work, we evaluated the stability behavior of the CS−GM and CS/TPP−GM systems, made with phosphorylated GM and non-phosphorylated KGM, in PBS pH 7.4. Under the experimental conditions of this study, we observed that the nonmodified CS/TPP nanoparticles suffered aggregation, followed by precipitation, immediately upon dilution with PBS. In contrast, the results presented in Figure 4 show that both non-phosphorylated KGM and phosphorylated GM have a positive effect in preserving the original size of the nanoparticles. However, it should also be noted from these results that, irrespective of the presence of TPP, the nanoparticles containing non-phosphorylated KGM were totally stable, whereas those containing phosphorylated GM suffered a certain increase in their size. The different stability of the nanoparticles containing phosphorylated GM and non-phosphorylated KGM could be justified by the different forces involved in the association of the two polymers with CS. As indicated above, the interaction of phosphorylated GM with CS is supposed to be driven by ionic forces, whereas that of KGM should be driven mainly by hydrophobic and hydrogen binding forces[17] which are less labile in high ionic force media.

On the other hand, in Figure 4 it can be seen that the incorporation of TPP in the CS−phosphorylated GM nanoparticles led to a further increase in their particle size upon incubation in PBS. Although no clear explanation can be given to this result, one could speculate about the possibility of a competition between TPP and phosphorylated GM for the CS amino groups, leading to the formation of poorly stable nanoparticles with a low GM content. Additionally, there is the possibility that the incorporation of TPP leads to the formation of a less compact and more swellable structure upon incubation in ionic media.

3.3. Association of Insulin and P1 Protein to the Nanoparticles. In a previous work, we have shown the feasibility of

Table 5. Process Yield and Association Efficiencies of Insulin-Loaded CS and CS−GM Nanoparticles (Mean ± SD, $n = 4$)

formulation	CS/TPP/GM (w/w)	process yield (%)	assoc efficiency (%)
CS/TPP	6/1/0	49 ± 2	83 ± 2
CS/phosphorylated GM	6/0/4.6	35 ± 6	37 ± 3
CS/TPP/phosphorylated GM	6/0.7/4.6	46 ± 2	75 ± 3
CS/KGM	6/0/6	48 ± 3	69 ± 6
CS/TPP/KGM	6/1/1.8	67 ± 8	88 ± 1

Table 6. Process Yield and Association Efficiencies of P1 Protein-Loaded CS and CS−GM Nanoparticles (Mean ± SD, $n = 4$)

formulation	CS/TPP/GM (w/w)	process yield (%)	assoc efficiency (%)
CS/TPP	6/1/0	24 ± 0.4	27 ± 3
CS/phosphorylated GM	6/0/4.6	39 ± 5	37 ± 4
CS/TPP/phosphorylated GM	6/1/4.6	60 ± 2	15 ± 6
CS/KGM	6/0/6	36 ± 4	11 ± 3
CS/TPP/KGM	6/1/1.8	30 ± 4	31 ± 3

CS−GM nanoparticles, obtained by GM coating of previously obtained CS/TPP nanoparticles, for the entrapment of P1 protein.[20] The results showed that the association efficiency was not dependent on the phase (CS or TPP) in which the protein was incorporated; however, it was very positively affected by the previous dissolution of the protein in phosphate buffer. Working with acidic proteins, i.e., insulin, BSA, tetanus toxoid, we have shown that their association to CS nanoparticles was improved by dissolving them into the alkaline TPP phase.[8,13,24] This was attributed to a facilitated ionic interaction between the protein (negatively ionized at high pH) and the positively charged CS molecules and also to the differences of solubility of the associated proteins at the different pHs. We decided to dissolve insulin and P1 protein in NaOH (0.01 M) and 10 mM phosphate buffer (pH 6.6), respectively, and to add them to TPP and/or GM solutions, which thereafter were mixed with the CS solution.

The results in Table 5 show that insulin was associated efficiently to all the developed formulations. In addition, it can be noted that the presence of TPP has a positive effect on the insulin association (37 and 69% vs 83, 75, and 88% for CS−phosphorylated GM, CS−KGM and CS/TPP, CS/TPP−KGM, CS/TPP−phosphorylated GM, respectively). This effect could be simply related to the increase of the pH in the medium where the protein was incorporated due to the presence of TPP. In fact, the pH of the TPP solution containing either phosphorylated GM or non-phosphorylated KGM was from 8.6 to 9.0, whereas that of the same solutions without TPP varied between 7.1 and 8.2. This dependence of the association efficiency of insulin to CS nanoparticles with the formulation pH was also reported by Ma et al.[30] In the more basic medium insulin is more negatively charged, and hence, its possibility to ionically interact with CS is improved.[31] Despite previous reports about the competition between polymers and proteins in their association to CS,[13,32] under the experimental conditions assayed, the association efficiency of insulin was not affected by the presence of KGM (comparison of formulations CS/TPP and CS/TPP−KGM). This may be due to the fact that there are enough free amine groups available in the CS molecules for the interaction with insulin. However, we found this competition for higher KGM content (data not shown).

According to the results depicted in Table 6, in general, P1 protein was less efficiently associated with the nanoparticles than insulin. Bearing in mind that one of the mechanisms of protein association to CS/TPP nanoparticles is mediated by protein−CS electrostatic interactions,[12] the different attachment of insulin and P1 could be explained on the basis of their different isoelectric point (IP) and ionization degree in the protein solutions. The IP of insulin is 5.3; however, P1 protein is a mixture of polypeptides with IP varying within 3 and 9. Thus, in the processing conditions of this study, insulin is negatively charged and, consequently, able to interact ionically with CS ($pK_a = 6.5$). In contrast, P1 protein is less negatively ionized, and hence, its ionic interaction with CS is reduced.

With regard to the association of P1 protein, as previously observed for insulin, there were no significant differences between the protein association to CS/TPP and CS/TPP−KGM nanoparticles (27 ± 3 and 31 ± 3, respectively). This indicates that non-phosphorylated KGM does not compete with the protein for CS in CS/TPP−KGM nanoparticles with theoretical ratio 6/1/1.8. However, as expected, the incorporation of higher amounts of non-phosphorylated KGM led to a decrease on the association efficiency (until a value of 10%, data not shown). This finding suggests that the competition between P1 protein and non-phosphorylated KGM occurs, only, for high KGM contents. This competition effect between protein P1 protein and GM was more pronounced in the case of phosphorylated GM. Indeed, the incorporation of higher amounts of phosphorylated GM to the nanoparticles resulted in a decrease in P1 protein association efficiency from 37% to 22%. This value was further reduced in the presence of TPP (37 vs 15%), indicating that a competition may occur as well between P1 and TPP. Consequently, overall these results suggest that the interaction of the fraction of P1, negatively charged, with CS may be interfered by TPP and GM.

In summary, as expected, insulin association is strongly influenced by the pH of the medium, being more important when the pH increases. In contrast, the association of P1 protein is not significantly affected by the pH, but by the presence of phosphorylated GM and TPP.

3.4. In Vitro Release of Insulin and P1 Protein from the Nanoparticles. Previous studies have shown that insulin is very rapidly released from the CS nanoparticles upon incubation at pH 7.4 PBS. These results suggested that the mechanism of release was a simple dissociation of the protein from the particles. More specifically, it was assumed that the presence of high ion concentrations in the media interfered with the electrostatic interactions that retained the protein within the nanoparticles, causing its fast release. In this study we aimed to investigate whether the presence of GM could affect this dissociation process. The formulations selected to perform these studies were CS−phosphorylated GM and CS−KGM nanoparticles with theoretical ratios of 6/4.6 and 6/6, respectively, and CS/TPP−phosphorylated GM and CS/TPP−KGM nanoparticles with theoretical ratios of 6/1/4.6 and 6/1/1.8, respectively. CS/TPP (6/1) nanoparticles were used as controls. The profiles plotted in Figure 5 reveal that insulin release was slower from the formulations containing non-phosphorylated KGM as compared to those without GM or containing phosphorylated GM. These results correlate well with those from the stability study and also suggest that the nanoparticles without GM or containing phosphorylated GM are more susceptible to the swelling or disassociation of the individual components. Moreover, the higher M_w and the lower solubility of KGM as compared to phosphorylated GM could make more difficult the diffusion of the peptide through the polymer networks into the release medium.[18,33] On the other hand, it can be noted that the presence of TPP in the CS−phosphorylated GM formulations reduces the release rate. This could be understood by the restricted

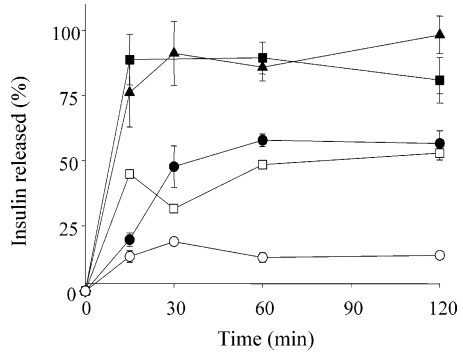

Figure 5. Release profiles of insulin from the nanoparticles in PBS pH 7.4 at 37 °C (CS/insulin: 2.4−2/1; mean ± SD, $n = 4$). Nanoparticles polymer composition: (▲) CS/TPP (6/1); (●) CS/TPP/phosphorylated GM (6/1/4.6); (■) CS/phosphorylated GM (6/4.6); (□) CS/KGM (6/6); (○) CS/TPP/KGM (6/1/1.8).

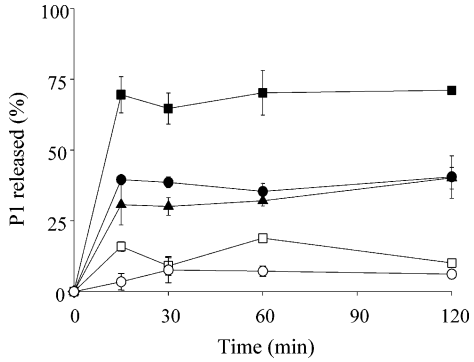

Figure 6. Release profiles of P1 protein from the nanoparticles in PBS pH 7.4 at 37 °C (CS/P1: 2.2−1.6/1; mean ± SD, $n = 4$). Nanoparticles polymer composition: (▲) CS/TPP (6/1), (●) CS/TPP/phosphorylated GM (6/1/4.6), (■) CS/phosphorylated GM (6/4.6), (□) CS/KGM (6/6) and (○) CS/TPP/KGM (6/1/1.8).

diffusion of the peptide through a highly CS cross-linked network, when it is ionically cross-linked with TPP, and reinforced by the presence of phosphorylated GM. Similar findings were found by Xu et al. for BSA loaded modified CS nanoparticles: the inclusion of PEG or sodium alginate gave slower release profiles.[26]

As in the case of insulin, the release of P1 protein was more rapid from the nanoparticles containing phosphorylated GM than from those made of non-phosphorylated GM (Figure 6). However, in this case, the release of P1 from CS nanoparticles occurred more slowly than insulin. This could be related to the molecular weight of P1 and the different interaction forces polymer−protein, which have been reported to affect the diffusion of proteins through the gelified nanostructure.[12] For this protein, the fastest release was observed for the formulation CS−phosporylated GM, which did not contain TPP. This result could be explained by the improved diffusion of P1 protein through a less cross-linked structure.

Overall, the in vitro protein release results suggest that there are possibilities of modulating the release rate of insulin and P1 protein by selecting the GM type and the GM and TPP content.

4. Conclusions

The preparation of various nanoparticulate systems composed of the hydrophilic polymers CS and GM is reported. These nanoparticles are formed under very mild conditions, and they have an excellent capacity for the association of the model proteins insulin and P1 protein. The protein release can be modulated by adequately selecting the type and content of GM. Furthermore, the nanoparticles are stable in pH 7.4 phosphate buffer. These interesting features make these nanoparticles very promising vehicles for oral administration of peptides and proteins and, more specifically, for their targeting to the M cells of Payer's patches.

Acknowledgment. This work was financed by the Spanish Government (FEDER 1FD97-2363, MCYT-AK22) and Industrial Farmacéutica Cantabria S.A. The first author acknolowledges the grant from the Spanish Government (FPU-MEC).

References and Notes

(1) Fix, J. A. *Pharm. Res.* **1996**, *13*, 1760−1764.
(2) Lipka, E.; Crison, J.; Amidon, G. L. *J. Controlled Release* **1996**, *39*, 121−129.
(3) Blanco, D.; Alonso, M. J. *Eur. J. Pharm. Biopharm.* **1998**, *45*, 285−294.
(4) Hirano, S.; Seino, H.; Akiyama, Y.; Nonaka, I. In *Progress in Biomedical Polymers*; Gebelein, C. G., Dunn, R. L., Eds.; Plenum Press: New York, 1990; p 283.
(5) Dornish, M.; Hagen, A.; Hansson, E.; Pecheur, C.; Verdier, F.; Skaugrud, Ø. In *Advances in Chitin Science*; Domard, A., Roberts, G. A. F., Vårum, K. M., Eds.; Jacques Andre Publishers: Lyon, 1997; p 664.
(6) Lehr, C. M.; Bouwstra, J. A.; Schacht, E. H.; Junginger, H. E. *Int. J. Pharm.* **1992**, *78*, 43−48.
(7) Borchard, G.; Luessen, H. L.; De Boer, G. A.; Coos Verhoef, J.; Lehr, C. M.; Junginger, H. E. *J. Controlled Release* **1996**, *39*, 131−138.
(8) Fernández-Urrusuno, R.; Calvo, P.; Remuñán-López, C.; Vila-Jato, J. L.; Alonso, M. J. *Pharm. Res.* **1999**, *16*, 1576−1581.
(9) De Campos, A.; Sanchez, A.; Alonso, M. J. *Int. J. Pharm.* **2001**, *224*, 159−168.
(10) Portero, A.; Remuñan-López, C.; Mørck Nielsen, H. *Pharm. Res.* **2002**, *19*, 169−174.
(11) Janes, K. A.; Calvo, P.; Alonso, M. J. *Adv. Drug Delivery Rev.* **2001**, *47*, 83−97.
(12) Calvo, P.; Remuñán-López, C.; Vila-Jato, J. L.; Alonso, M. J. *J. Appl. Polym. Sci.* **1997**, *63*, 125−132.
(13) Calvo, P.; Remuñán-López, C.; Vila-Jato, J. L.; Alonso, M. J. *Pharm. Res.* **1997**, *14*, 1431−1436.
(14) Vila, A.; Sanchez, A.; Janes, K.; Behrens, I.; Kissel, T.; Vila Jato, J. L.; Alonso, M. J. *Eur. J. Pharmacol. Biopharm.* **2004**, *57*, 123−131.
(15) Tomizawa, H.; Aramaki, Y.; Fujii, Y.; Kara, T.; Suzuki, N.; Yachi, K.; Kikuchi, H.; Tsuchiya, S. *Pharm. Res.* **1993**, *10*, 549−552.
(16) Cui, Z.; Hsu, Ch.; Mumper R. J. *Drug Dev. Ind. Pharm.* **2003**, *29*, 689−700.
(17) Xiao, Ch.; Gao, S.; Wang, H.; Zhang, L. *J. Appl. Polym. Sci.* **2000**, *76*, 509−515.
(18) Wang, K.; He, Z. *Int. J. Pharm.* **2002**, *244*, 117−126.
(19) Paulesu, L.; Pessina, G. P.; Nocoletti, C.; Boccanera; M.; Cassone, A. *Immunol. Lett.* **1991**, *27*, 231−235.
(20) Cuña, M.; Alonso-Sande, M.; Remuñán-López, C.; Pivel, J. L.; Alonso-Lebrero, J. L.; Alonso, M. J. *J. Nanosci. Nanotechnol.*, in press.
(21) Schazt, C.; Pichot, C.; Delair, T.; Viton; C.; Domard, A. *Langmuir* **2003**, *19*, 9896−9903.
(22) Tsaih, M.; Chen, R. H. *J. Appl. Polym. Sci.* **1999**, *73*, 2041−2050.
(23) Signini, R.; Desbrières, J.; Campana Filho, S. P. *Carbohydr. Polym.* **2000**, *43*, 351−357.
(24) Janes, K.; Alonso, M. J. *J. Appl. Polym. Sci.* **2003**, *88*, 2769−2776.
(25) Du, J.; Sun, R.; Zhang, S.; Govender, T.; Zhang, L. F.; Xiong, Ch. D.; Peng, Y. X. *Macromol. Rapid Commun.* **2004**, *25*, 954−958.
(26) Xu, Y.; Du, Y.; Huang, R.; Gao, L. *Biomaterials* **2003**, *24*, 5015−5022.
(27) Schatz, C.; Domard, A.; Viton, C.; Pichot, C.; Delair, T. *Biomacromolecules* **2004**, *5*, 1882−1892.
(28) Thu, B.; Bruheim, P.; Espevik, T.; Smidsroed, O.; Soon-Shiong, P.; Skjak-Braek, G. *Biomaterials* **1996**, *17*, 1031−1040.
(29) Vila, A.; Sánchez, A.; Tobío, M.; Calvo, P.; Alonso, M. J. *J. Controlled Release* **2002**, *78*, 15−24.
(30) Ma, Z.; Yeoh, H. H.; Lim, L. Y. *J. Pharm. Sci.* **2002**, *91*, 1396−1404.
(31) Yoshida, H.; Nishihara, H.; Kataoka, T. *Biotechnol. Bioeng.* **1994**, *43*, 1087−1093.
(32) Xu, Y.; Du Y. *Int. J. Pharm.* **2003**, *250*, 215−226.
(33) Nakano, M.; Takikawa, K.; Arita, T. *J. Biomed. Mater. Res.* **1979**, *13*, 811−819.

MA060230J